PROFESSOR MICHAEL HICKEY (Orcid ID : 0000-0003-2354-357X)

PROFESSOR WEISAN CHEN (Orcid ID : 0000-0002-5221-9771)

Article type : Original Article

Memory regulatory T cells home to the lung and control influenza A virus infection

Chunni Lu[1], Damien Zanker[1], Peter Lock[1], Xiangrui Jiang[1], Jieru Deng[1], Mubing Duan[1], Chuanxin Liu[1], Pierre Faou[1], Michael J Hickey[2] and Weisan Chen[1,3]

[1]La Trobe Institute for Molecular Science, School of Molecular Science, La Trobe University, Bundoora, VIC, Australia.

[2]Centre for Inflammatory Diseases, Monash University Department of Medicine, Monash Medical Centre, Clayton, VIC, Australia.

Running title: Memory Tregs control influenza A virus infection in the lung

Keywords: Influenza A virus, infection-experienced, memory regulatory T cells, C57BL/6

[3]To whom correspondence should be addressed: weisan.chen@latrobe.edu.au

ABSTRACT

Memory regulatory T cells (mTregs) have been demonstrated to persist long-term in hosts after the resolution of primary influenza A virus (IAV) infection. However, whether such IAV infection-experienced (IAV-experienced) mTregs differentiate into a phenotypically and functionally distinct Treg subset and what function they play at the infection site remain poorly defined. In this study, we characterized the phenotype, examined the responsiveness and assessed the suppressive function of IAV-experienced mTregs. In comparison with inexperienced naïve Tregs (nTregs), mTregs exhibited elevated expression of CD39, CD69, CD103, CTLA-4, LFA-1 and PD-1 and could be activated in an antigen-specific manner *in vitro* and *in vivo*. When mTregs and nTregs were adoptively co-transferred into recipient mice, mTregs had a competitive advantage in migrating to the IAV infected lungs. mTregs were more capable of controlling *in vitro* proliferation of $CD4^+$ and $CD8^+$ T cells and suppressed CD40 and CD86 upregulation on bone marrow-derived dendritic cells (BMDCs). Adoptively transferred mTregs, but not nTregs, significantly attenuated body weight loss, lung pathology and immune cell infiltration into the infected lungs. These results suggest that mTregs generated after IAV infection differentiate into a phenotypically distinct and functionally enhanced Treg subset that can be activated in an antigen-specific manner to exert immunosuppression. We propose vaccination to induce such mTregs as a potential novel strategy to protect against severe IAV infection.

INTRODUCTION

Regulatory T cells (Tregs) expressing the X-chromosome-encoded transcription factor Foxp3 represent a specialized lineage of T lymphocytes with prominent immunosuppressive function.[1, 2] Tregs were initially discovered as a key immunoregulator of autoimmunity, maintaining self-tolerance via suppressing autoreactive T cells that have escaped negative selection in thymus.[3, 4]

Imbalance between Tregs and autoreactive T cells, impaired Treg proliferation capacity or defects in Treg suppressive function may therefore lead to the development of a variety of autoimmune diseases.[5-8] In addition to the maintenance of immune tolerance to self-antigens, Tregs are involved in modulating immune responses to acute microbial pathogens. For example, during acute infection by respiratory syncytial virus (RSV) and herpes simplex virus (HSV), Tregs are critical in limiting the infection-induced innate and adaptive immune responses and the corresponding tissue inflammation at the infection sites.[9-12]

Tregs have been investigated in acute influenza A virus (IAV) infection in recent years. It has become clear that, following primary IAV infection, Tregs can be activated by IAV-derived peptides and the activated Tregs are widely disseminated in the lung and lung-draining mediastinal lymph node (mLN) and, to a lesser extent, in the spleen and peripheral non-draining lymph node (pLN).[13, 14] Importantly, after the resolution of primary IAV infection, Tregs could maintain within the host to become long-lived memory Tregs (mTregs).[15] However, whether such IAV-infection experienced (IAV-experienced) mTregs represent a distinct Treg subset that differs from the inexperienced naïve Tregs (nTregs) in their phenotypes and their roles during subsequent IAV infection are largely unclear. The persistence of IAV-experienced mTregs in the host may point to a potential vaccination strategy, inducing a pool of IAV-experienced mTregs to target a wide range of IAV infection-induced detrimental cellular immune responses. However, the therapeutic efficacy of such IAV-experienced mTreg remains to be determined.

In this study, we sought to address these questions by deciphering the phenotype and examining the responsiveness and suppressive capacity of IAV-experienced mTregs. Considering that the appropriate localization of Tregs at the infection site is essential for them to interact with and modulate their cellular targets,[16] we also evaluated the ability of IAV-experienced mTregs to migrate into the infected lungs and their effects on IAV infection-induced pulmonary cellular immune responses. We found that mTregs exhibited elevated expression of cell migration- and function-associated molecules relative to nTregs. Upon activation *in vitro*, mTregs displayed enhanced proliferation and cytokine production capacity compared to nTregs. In response to IAV infection *in vivo*, mTregs were highly activated, proliferative and showed competitive advantage in migrating to the infection site in comparison with nTregs. Importantly, mTregs could effectively attenuate lung pathology, limit pulmonary immune cell infiltration and control

ongoing antigen-specific T cell responses in the lungs. These data suggest that mTregs generated in the setting of IAV infection have differentiated into a population with distinct phenotype, enhanced responsiveness and peripheral infection-site migratory capacity which give rise to their control of IAV infection.

RESULTS

mTregs display distinct phenotype and are more responsive to IAV than nTregs in vitro

Knowing that a pool of mTregs can be differentiated and maintained in the host after the resolution of primary IAV infection,[15] we questioned whether mTregs are phenotypically different from their naïve counterparts. To address this question, we analyzed the phenotype of nTregs and mTregs from various tissues including spleen, peripheral non-draining inguinal lymph node (pLN), lung-draining mediastinal lymph node (mLN) and lung of IAV-infected mice. Considering that the bulk of mTregs may contain a small fraction of Tregs with $CD44^{+}CD62L^{-/low}$ phenotype that was also found in naïve mice,[17] we therefore included Tregs with $CD44^{+}CD62L^{-/low}$ expression from age/sex matched naïve mice, termed them as "nmTregs", as control. We assessed the expression of surface molecules associated with cell activation, proliferation and migration, including CD25, CD39, CD69, CD103, cytotoxic T lymphocyte-associated antigen-4 (CTLA-4), leukocyte function-associated antigen-1 (LFA-1), programmed cell death-1 (PD-1) and Foxp3. Our results showed that the expression levels of Foxp3 on nTregs and mTregs were similar, whereas the CD25 expression on mTregs was slightly lower (Figure 1). Noteworthily, mTregs exhibited elevated expression of an array of cell migration- and suppressive function-associated molecules, including CD39, CD69, CD103, CTLA-4, LFA-1 and PD-1 (Figure 1). Thus, mTregs represent a distinct Treg population.

We further determined whether mTregs could actively respond to IAV *in vitro* by investigating cell activation and proliferation marked by Ki67 expression. Nearly 38% mTregs stimulated with IAV-infected BMDCs expressed Ki67, but only 10% of nTregs expressed Ki67 (Figure 2a). Moreover, tracking nTregs and mTregs via time-lapse live cell imaging revealed that, after being co-cultured with IAV-infected BMDCs, mTregs but not nTregs displayed frequent change in cell morphology and made more contact with IAV-infected BMDCs (Figure 2b and Supplementary

figure 1a and b), which suggests that mTregs were more activated and more mobile than nTregs. To show the lack of nTreg response was not an intrinsic defect in these cells, we stimulated both mTregs and nTregs using anti-CD3/CD28 mAbs and more than 90% mTregs and nTregs expressed the proliferation marker Ki67 (Supplementary figure 2), indicating these Tregs are equally capable of responding to TCR stimulation.

mTregs are highly activated and proliferative upon IAV infection with an enhanced infection site-migration capacity

We next sought to understand the extent to which mTregs differ from their naïve counterparts in responding to IAV *in vivo*. We co-transferred mTregs isolated from IAV-immunized C57BL/6 Foxp3^{eGFP} mice and nTregs isolated from uninfected C57BL/6 mice into congenic Ly5.1 recipients (Figure 3a), so that the responsiveness of mTregs and nTregs to IAV could be directly compared in the same environment. The recipients were intranasally infected with IAV 12 h after co-transfer. The distribution, activation and proliferation of the adoptively co-transferred mTregs (eGFP$^+$ and CD45.2$^+$) and nTregs (eGFP$^-$ and CD45.2$^+$) were investigated 10 days post infection (dpi) (Figure 3b). At 10 dpi, both the co-transferred mTregs and nTregs were detected in the spleens, pLNs, mLNs, BALs and lungs of the recipients. However, mTregs were highly activated and more proliferative than nTregs in all of the analyzed tissues based on Ki67$^+$ cell proportion (Figure 3c). Moreover, the proportions of mTregs were higher than that of nTregs in the spleens and much more so in the BALs (93% vs 7%) and lungs (86% vs 14%) (Figure 3d). These observations were consistent with their numbers in all analyzed tissues, with higher number of mTregs than nTregs in the spleens, BALs and lungs and comparable numbers of both populations in the pLNs and mLNs (Figure 3e). Thus, mTregs are specifically activated *in vivo* upon exposure to IAV and have a competitive advantage in migrating to and proliferating at the infection site during IAV infection, which was further supported by the lack of proliferation and much lower migration number in the above-mentioned sites when transferred mTregs were tracked in mice treated with PBS (Supplementary figure 3).

mTregs are more capable of inhibiting T cell proliferation and modulating BMDC costimulatory function in vitro than nTregs

We next assessed the suppressive capacity of these various Treg subsets *in vitro* in a $CD4^+$ or $CD8^+$ T cell proliferation assay. Infected antigen presenting cells are considered as a more physiological APC to evaluate Treg suppression [15]. Thus, mTregs or nTregs were cocultured with IAV-specific $CD4^+$ and $CD8^+$ T cells stimulated by IAV-infected BMDCs. Our results showed that both IAV-specific $CD4^+$ and $CD8^+$ T cells were highly proliferative when they were stimulated with IAV-infected BMDCs in the absence of mTregs or nTregs (Figure 4a and b). When mTregs or nTregs were added into the co-cultures, the proliferation of IAV-specific $CD4^+$ and $CD8^+$ T cells were significantly inhibited (Figure 4c). Suppressive effects of nTregs and mTregs closely correlated with Treg/responder T cell ratio, with increased suppression on IAV-specific $CD4^+$ and $CD8^+$ T cell proliferation at higher Treg/responder T cell ratios. In comparison to nTregs, mTregs displayed 2~4 fold enhanced suppression on IAV-specific $CD4^+$ and $CD8^+$ T cell proliferation on a per cell basis (Figure 4c). Thus, mTregs are more capable of suppressing IAV-specific $CD4^+$ and $CD8^+$ T cells proliferation.

We also examined whether mTregs could regulate the T cell stimulatory function of BMDCs by analyzing their expression of core functional molecules, CD40, CD86 and MHC-II. BMDCs co-cultured with IAV-specific $CD4^+$ T cells in the presence of IAV showed dramatic upregulation in their co-stimulatory molecule CD40 and CD86 expression compared with control BMDCs cultured in medium alone (Figure 5a and b). However, such co-stimulatory molecule upregulation was dramatically reduced when mTregs were added into the co-cultures (Figure 5a and b), nTregs showed significantly less suppression on CD40 and CD86 expression compared to mTregs (Figure 5a and b). Notably, the evident up- or down-regulation of CD40 and CD86 on BMDCs were observed only when BMDCs were co-cultured with $CD4^+$ T cells or $CD4^+$ T cells plus Tregs, respectively, in the presence of IAV, as there was no significant increase in CD40 or CD86 expression on BMDCs cultured in the presence of IAV compared to BMDCs cultured in medium alone (Supplementary figure 4a and b). MHC-II expression on BMDCs was not altered either co-cultured with or without T cells, plus or minus nTregs or mTregs (data not shown). Collectively, these data suggest that mTregs actively control T cell costimulation function of

BMDCs through suppressing their CD40 and CD86 up-regulation, and such control by mTregs is more potent than that by nTregs.

mTregs effectively attenuate IAV infection-induced body weight loss and lung pathology

We next sought to define a role for mTregs *in vivo* during IAV infection. Intranasal infection with a sublethal dose of IAV generally result in body weight loss and lung tissue damage in mice. In our study, mice that were intranasally infected by a sublethal dose of PR8 displayed a progressive reduction in body weight between 3-9 days post infection (Figure 6a, "Infected"). Moreover, histopathological analysis and histology scoring of the infected lungs at 10 dpi revealed extensive cell infiltration in the lung parenchyma and a markedly increased severity of overall lung pathology compared to the uninfected lungs (Figure 6a and c, "Infected only"). Interestingly, however, the adoptively transferred mTregs actively attenuated infection-induced body weight loss, coupled with an earlier recovery of body weight from day 8 post infection (Figure 6a, blue line). The presence of adoptively transferred mTregs also significantly attenuated the prominent lung immune cell infiltration and pathology (Figure 6b and c, "Infected + mTregs"). To account for a potential contribution of nTregs, we also infected recipient mice received adoptively transferred nTregs. Nevertheless, under the same conditions, nTregs failed to ameliorate such infection-induced body weight loss (Figure 6a, "Infected + nTregs") and lung pathology (Figure 6b and c, "Infected + nTregs"). Thus, these data together demonstrate a key role for mTregs in controlling IAV infection-induced body weight loss and mediating tissue protection during IAV infection.

mTregs selectively limit the infiltration of monocytes and neutrophils into the infected lungs

To understand how mTregs contribute to the control of IAV infection-induced lung pathology, we analyzed the infiltrating cells in the lungs of mice that had or had not received mTregs. During IAV infection, while innate and adaptive immune cells rapidly orchestrate antiviral immune responses to control the infection, they may also act deleteriously to initiate or exacerbate the production of pro-inflammatory cytokines and chemokines, reactive oxygen species and nitric oxide that may lead to lung tissue injury.[18, 19] Therefore, we analyzed the lung-

infiltrating monocytes, interstitial macrophages, neutrophils, IFN-γ-secreting $CD4^+$ and $CD8^+$ T cells at 10 dpi. Our results showed that IAV infection led to a dramatic increase of the infiltration of these cell types into the lungs (Supplementary figure 5, "Infected only"). However, in mice that received mTreg transfer, IFN-γ-secreting $CD4^+$ and $CD8^+$ T cell infiltration was markedly reduced, and monocyte and neutrophil infiltration was significantly reduced (Supplementary figure 5, "Infected + mTregs"). In mice that received nTregs, such infiltration was largely unaffected (Supplementary figure 5, "Infected + nTregs"). Collectively, these data suggest that mTregs mediate lung tissue protection most likely by limiting immune cell infiltration, especially monocytes and neutrophils, into the lung.

DISCUSSION

We showed in this study that IAV-experienced mTregs belong to a distinct Treg subset. In fact, our study provides the first comprehensive phenotyping of IAV-experienced mTregs. We further demonstrated that IAV-experienced mTregs, but not nTregs, are more responsive *in vitro* to IAV-infected APCs and able to suppress the upregulation of BMDC costimulation molecules; and that *in vivo* they are more capable of migrating into IAV infection site, proliferating vigorously, suppressing innate and adaptive immune cell infiltrating into the infected lungs, and most importantly attenuating lung pathology caused by IAV infection reflected by both much milder histological changes and significantly decreased body weight loss.

A previous study investigating Treg regulation of memory $CD8^+$ T cell response to secondary IAV infection revealed the long-term existence of mTregs in the host.[15] However, the phenotypical difference between IAV-experienced mTregs and their naïve counterparts is not well established. We have shown in this study that the expression of CD39, CD69, CD103, CTLA-4, LFA-1 and PD-1 is upregulated in mTregs as opposed to nTregs, providing further evidence for the previously identified mTregs in the setting of IAV infection that IAV-experienced mTregs have differentiated into a phenotypically distinct subset of Tregs.

Tregs become activated in response to IAV infection and were shown to play an important role in modulating immune responses to primary IAV infection,[14, 20, 21] and mTregs were shown to be

more capable of suppressing pulmonary $CD8^+$ T cell response during secondary IAV infection than nTregs.[15] Interestingly, the factors that contribute to such enhanced immunosuppression of mTregs during IAV infection remain poorly understood as both nTregs and mTregs should have similar suppression capacity on a per cell basis.[22] However, since Tregs must be activated to exert their suppressive function,[23] one possible mechanism is that mTregs are able to recognize previously encountered antigens. This may confer an enhanced ability of mTregs to search and interact with APCs bearing previously encountered IAV antigens for activation and proliferation, especially at the infection site. In support for this, we compared the responsiveness of mTregs and nTregs *in vitro* and *in vivo* and found that mTregs, but not nTregs, were highly activated *in vitro* after stimulation with IAV-infected BMDCs. Time-lapse live cell imaging also showed that mTregs were more capable of interacting with IAV-infected BMDCs. Moreover, in IAV-infected recipient mice, significantly more transferred mTregs were activated than nTregs in all analyzed tissues, including spleens, pLNs, mLNs, BALs and, especially in the lungs. Such activation was largely antigen-specific as only a small fraction of the transferred mTregs were activated in the uninfected recipients. Another possible mechanism could be the mTregs' enhanced infection site-migration capacity. There is increasing evidence indicating that appropriate Treg migration is essential for them to interact with and modulate their cellular targets. For example, CD62L expressing Tregs were especially potent at entering lymph nodes to suppress proliferation of self-antigen- and alloantigen-specific T cells, thereby suppressing autoimmunity and graft rejection, respectively.[24, 25] In contrast, CD103 expressing Tregs displayed poor capacity in migrating to lymph nodes but were exclusively recruited to skin to control Leishmania major infection and antigen-induced arthritis.[26, 27] The elevated expression of CD103 on mTregs, relative to that on nTregs, therefore indicate an enhanced infection site-migration capacity of mTregs. Consistent with this possibility, after adoptive co-transfer, we found significantly more mTregs than nTregs in the BALs and lungs of infected recipients at 10 dpi.

Two mechanisms may be involved in mTregs-mediated attenuation of lung pathology and body weight loss. Firstly, this could be the outcome of decreased pulmonary immune cell infiltration as in mice that had received mTregs the infiltrating monocytes, neutrophils and IFN-γ-producing $CD4^+$ and $CD8^+$ T cells were significantly reduced. These cells secreted proinflammatory cytokines such as TNF-α, IL-1β and IL-6 following IAV infection,[19] and they were reported to contribute to "cytokine storm".[28-30] Since monocytes are the major source of chemoattractant

MIP-1α, MCP-1 and IP-10 [31], the suppression of pulmonary infiltration of monocytes by mTregs may prevent recruitment of additional immune cells to the infected lungs, thereby the exacerbation of lung pathology. Secondly, the higher expression of CD39 by mTregs may contribute to tissue protection. In support of this conclusion, CD39 expressed by Tregs was shown to induce the production of immunosuppressive adenosine through hydrolyzing proinflammatory ATP, thereby controlling IL-17 mediated autoimmune inflammation and the secretion of proinflammatory cytokine IL-1β.[32, 33]

We observed that there were significant reductions in the numbers of IFN-γ-producing $CD4^+$ and $CD8^+$ T cells in the infected lungs of mice that had adoptively transferred mTregs. Such suppression of IFN-γ-producing $CD4^+$ and $CD8^+$ T cell responses in the lungs by mTregs may be mediated by modifying the antigen-presentation capacity of local APCs. It has been reported that additional antigen presentation by pulmonary APCs, including plasmacytoid DCs, $CD8\alpha^+$ DCs and interstitial DCs, sustains antigen-specific T cell responses in the infected lungs.[34] However, CTLA-4 expressed by Tregs was demonstrated to limit T cell priming and proliferation via suppressing co-stimulation function of DCs.[35, 36] In addition, aggregation of Tregs on DCs in an LFA-1 dependent-manner also led to a lethargic state of DCs, thereby a reduced T cell priming.[37] We also observed that mTregs had markedly elevated expression of CTLA-4 and LFA-1 compared to nTregs. More importantly, mTregs could actively down-regulate CD40 and CD86 expression on BMDCs. Therefore, mTregs may actively act on pulmonary APCs leading to the inhibition of excessive antigen-specific $CD4^+$ and $CD8^+$ T cell responses.

Taken together, using an adoptive Treg transfer approach, rather than $CD25^+$ Treg depletion, we demonstrate an IAV-experienced mTreg population, likely containing polyclonal IAV-specific mTregs, was able to reduce IAV-infection associated lung pathology and body weight loss. Our study model resembles a preventative vaccination scenario in which an antigen-specific mTreg pool was established before the host was IAV infected. IAV-specific mTregs can be induced after vaccination with UV-inactivated IAV or vaccines containing specific IAV peptides, although such Tregs may dampen the effector T cell response a little.[38, 39] It is possible and likely helpful that for future IAV vaccines to incorporate specific strategies to stimulate some IAV-specific mTregs. It would be more appealing if such vaccine is given via the intranasal route and induces lung-resident mTregs as intranasal administration but not injection of influenza vaccines

are more expected to improve the efficacy of influenza vaccines and generating lung-resident memory T cells.[40, 41] Such IAV-specific mTregs or lung-resident mTregs might provide more timely immune regulation at the infection sites to minimize IAV infection-caused immunopathology without significantly affecting immune protection provided by both innate and adaptive immune cells.

METHEODS

Mice

Female C57BL/6 and Ly5.1 mice were purchased from the Walter Eliza Hall Institute of Medical Research (Melbourne, Australia). B6-Foxp3^{eGFP} mice, on a C57BL/6 background,[42] were kindly provided by Dr. Alexander Y. Rudensky (Memorial Sloan Kettering Cancer Center, New York, NY) and bred in house. Mice were housed under specific pathogen free (SPF) conditions in the animal facility at La Trobe University. All animal experiments were approved by the La Trobe University Animal Ethics Committee and performed in accordance with the National Health and Medical Research Council guidelines.

Influenza A viruses and infections

Influenza A virus PR8 (A/Puerto Rico/8/34, H1N1) was obtained from Lorena Brown (University of Melbourne, Australia) and X-31 (A/X-31, H3N2) from Jonathan Yewdell (NIH, USA). New viral stocks of PR8 and X-31 were propagated in 10-day-old embryonated chicken eggs, titered and stored as previously described.[43] For *in vivo* primary infection, 9~10-week-old mice were anesthetized with methoxyflurane and intranasally infected with 70 pfu of PR8 (in 30 µl PBS). For *in vivo* secondary infection, mice were firstly infected by 70 pfu of PR8 and challenged 35 days later with 10^4 pfu of X-31 (in 30 µl PBS). For *in vitro* infection, 1~3 x 10^6 cells were co-incubated with a 10 multiplicity of infection (MOI) dose of PR8 for 1 h in 200 µl AIM medium (RPMI-1640 medium supplemented with HCl to pH 6.0), followed by 12 h in 2 mL complete medium, RPMI-1640 medium supplemented with 10% fetal calf serum (FCS), at 37°C, 5% CO_2.

Tissue harvest and cell isolation

Mice were sacrificed at indicated time points and cells were isolated from the spleens, lymph nodes, lung airways and lung parenchyma. Spleens were mechanically disrupted in incomplete medium (RPMI-1640 medium supplemented with 2% FCS). Lymph nodes were mechanically disrupted in incomplete medium containing 5mM EDTA. Bronchoalveolar lavage (BAL) cells were collected by four instillations of BAL with 0.5 mL incomplete medium. Cells from the lung parenchyma were isolated by digestion with collagenase A and DNase I (1 mg mL^{-1} and 0.2mg mL^{-1}, respectively, Roche, Switzerland) at room temperature (RT) for 25 min prior to being passed through a nylon mesh. After red blood cell (RBC) lysis, cells were resuspended in complete medium before use.

Peptide stimulation

For *ex vivo* analysis of IFN-γ production by $CD4^+$ and $CD8^+$ T cells in the lungs, the cells isolated from the lungs were stimulated with peptides ($HA_{211-225}$, $NP_{311-325}$, $PB2_{106-120}$, and $PA_{465-470}$, 10^{-5} M, for $CD4^+$ T cell stimulation; $NP_{366-374}$, $PA_{224-233}$, $PB1_{703-711}$ and $PB2_{196-206}$, 10^{-8} M, for $CD8^+$ T cell stimulation) for 5 h in the presence of BFA at 37°C, 5% CO_2.

Cell staining and Flow cytometry

For cell surface marker staining, cells were incubated with Fc block (2.4G2, anti-CD16/32) for 10 min at 4°C. Without wash, cells were then stained with fluorescence-tagged antibodies, such as mAbs to CD3 (145-2C11), CD8 (53-6.7), CD11c (HL3), CD11b (M1/70), CD25 (PC61), CD40 (3/23), CD44 (IM7), CD45.1 (A20), CD45.2 (104), CD62L (MEL-14), CD69 (H1.2F3), CD86 (GL1), CD103 (M290), CD127 (SB/199), Ly-6G (1A8) and Siglec-F (MR1) purchased from BD Biosciences and CD4 (GK1.5), CD39 (24DMS1), LFA-1 (M17/4), Ly-6C (HK1.4), MHC-II (I-A/I-E) (M5/114.15.2) and PD-1 (J43) purchased from eBiosciences, at 4°C for 20~30 min. For intracellular staining of Foxp3, Ki67 and CTLA-4, cells were fixed in 1x Fixation/Permeabilization Buffer (eBiosciences) at 4°C for 45 min, followed by intracellularly

staining with mAbs to Foxp3 (MF23, BD Biosciences), Ki67 (SolA15, eBiosciences) or CTLA-4 (UC10-4B9, eBiosciences) in 1x Permeabilization Buffer (eBiosciences) for at least 1 h at 4°C. For intracellular cytokine staining (staining for IFN-γ and IL-10), cells were fixed in 1% paraformaldehyde (PFA) at RT for 30 min and then stained with mAbs to IFN-γ (XMG1.2, BD Biosciences) or IL-10 (JES5-16E3, Biolegend) in PBS containing 0.2% saponin at 4°C for 30 min. After being washed once with PBS, cell samples were resuspended 150 µl FACS buffer and acquired on a FACSCanto II flow cytometer (BD Biosciences). Flow cytometry data were analyzed with FlowJo software (FlowJo VX).

Cell sorting

Cell sorting was performed using a FACSAria III cell sorter (BD Biosciences). Memory $CD4^+$ T cells and $CD8^+$ T cells were FACS-sorted from the spleen and lymph node cells of memory C57BL/6 or Ly5.1 mice. Naïve and memory Tregs (nTregs and mTregs) were sorted from naïve and memory B6-$Foxp3^{eGFP}$ mice, respectively. Both nTregs and mTregs were $CD4^+CD25^+$ $Foxp3^{eGFP+}$; however, nTregs were $CD44^-CD62L^+$ and mTregs were $CD44^+CD62L^{-/low}$. For some experiments, $CD4^+CD25^+CD44^-CD62L^+$ nTregs and $CD4^+CD25^+CD44^+CD62L^{-/low}$ mTregs were sorted from naïve and memory C57BL/6 mice, respectively, by staining with mAbs to CD4, CD25, CD44 and CD62L. The cells isolated from Ly5.1 mice were $CD45.1^+$ and those isolated from C57BL/6 and B6-$Foxp3^{eGFP}$ mice were $CD45.2^+$.

Adoptive cell transfer

For *in vivo* Treg migration and proliferation analysis, FACS-sorted mTregs (1 x 10^6, $CD45.2^+eGFP^+$) were co-transferred with nTregs (1 x 10^6, $CD45.2^+eGFP^-$) into congenic Ly5.1 mice via tail intravenous injection (i.v.), followed by intranasal infection with PR8 (70 pfu in 30µl PBS) 12 h after co-transfer. For *in vivo* analysis of Treg function, nTregs (1.5~2 x 10^6, $CD45.2^+eGFP^+$) or mTregs (1.5~2 x 10^6, $CD45.2^+eGFP^+$) were i.v. transferred individually into congenic Ly5.1 recipient mice 12 h before intranasal PR8 infection.

Generation of BMDCs

2 x 10^6 bone marrow cells from naïve Ly5.1 or C57BL/6 mice were grown in complete medium supplemented with X-63-GM-CSF supernatant (containing granulocyte-macrophage colony-stimulating factor, GM-CSF) in 10 mm petri dish. Culture medium was replaced on day 3 and day 6. Bone marrow derived dendritic cells (BMDCs) were harvested on day 8 by collecting the nonadherent cells.

In vitro suppression assay

For *in vitro* suppression of T cell proliferation, the responder IAV-specific $CD4^+$ or $CD8^+$ T cells ($CD45.1^+$) were labeled with 5μM CFSE and cultured with Treg cell populations ($CD45.2^+$) at various ratios in the presence of irradiated PR8-infected BDMCs ($CD45.2^+$). IAV-specific $CD4^+$ or $CD8^+$ T cell proliferation was measured by carboxyfluorescein-succinimidyl ester (CFSE) dilution on day 5 and day 4 of culture, respectively. For *in vitro* suppression of BMDC activation, nTregs, mTregs or IAV-specific $CD4^+$ T cells (1 x 10^5, $CD45.2^+$) or a mix of two populations (1:1 ratio) were cultured with BMDCs (5 x 10^4, $CD45.1^+$) in U-bottomed 96-well plates in the presence of PR8 (MOI=1). After 24 h, cells were harvested by treating with 5 mM EDTA, and the expression of CD40, CD86 and MHC-II on BMDCs were FACS-analyzed after staining with mAbs specific to CD45.1, CD11c, CD86, CD40, and MHC-II.

Confocal microscopy

FACS-sorted nTregs and mTregs were labeled with Cell Proliferation Dye eFluor™ 670 and CFSE, respectively, according to the manufacturer's instruction. Labeled nTregs and mTregs (1.5 x 10^5) were cultured with non-labeled PR8-infected BMDCs (3 x 10^4) in 8-well Lab-Tek™ II Chambered Coverglass. Alternatively, labeled nTregs and mTregs (1.5 x 10^5) were cultured with non-labeled BMDCs (3 x 10^4) in the absence or presence of purified anti-CD3/anti-CD28 mAbs (1 μg mL^{-1} and 0.5 μg mL^{-1}, respectively). Live cell imaging was performed to analyze Treg-BMDC aggregation after 12 h co-incubation with a Zeiss Confocal Spinning Disk microscope. Cells were monitored with 20x and 63x objectives for analysis of cell aggregation

and morphological change, respectively. During imaging, cells were maintained at 37°C and supplemented with 5% CO_2 to sustain their viability.

Histological analysis

Recipient mice were adoptively transferred with nTregs or mTregs and infected with PR8 as previously described. Their lungs were collected on day 10 post infection and inflated with 1 mL PFA (4%, v/v) via the trachea and fixed for 16 h, at RT, followed by further fixation in 70% ethanol for 7 days at RT. Lungs were embedded in paraffin wax, and 5 mm sections were mounted onto slides and stained with H&E. All slides were imaged on a Nikon Eclipse microscope and captured images were analyzed by Fiji ImageJ software. The histology scores were assessed based on the infiltration rate calculated by Fiji ImageJ software.

Statistical analysis

Statistical analysis was performed using Prism 8 (GraphPad Software). Data are presented as mean ± SEM unless otherwise noted. Significance calculations were determined by unpaired two-tailed Student's *t*-test for comparison between two groups or one-way ANOVA for multiple comparisons between different groups. A value of $P > 0.05$ was deemed not statistically significant (ns); $*P < 0.05$, $**P < 0.01$, $***P < 0.001$, and $****P < 0.0001$.

ACKNOWLEDGMENTS

This project was partly supported by the NHMRC Senior Research Fellowship 603104 to WC and the NHMRC program grant 567122.

CONFLICT OF INTEREST

The authors declare no conflict of interest.

REFERENCES

1. Fontenot JD, Gavin MA, Rudensky AY. Foxp3 programs the development and function of $CD4^+CD25^+$ regulatory T cells. *Nat Immunol* 2003; **4:** 330-336.
2. Josefowicz SZ, Lu LF, Rudensky AY. Regulatory T cells: mechanisms of differentiation and function. *Annu Rev Immunol* 2012; **30:** 531-564.
3. Wing K, Sakaguchi S. Regulatory T cells exert checks and balances on self tolerance and autoimmunity. *Nat Immunol* 2010; **11:** 7-13.
4. Sakaguchi S, Yamaguchi T, Nomura T, *et al*. Regulatory T cells and immune tolerance. Cell 2008; **133:** 775-787.
5. Grant CR, Liberal R, Mieli-Vergani G, *et al*. Regulatory T-cells in autoimmune diseases: challenges, controversies and--yet--unanswered questions. *Autoimmun Rev* 2015; **14:** 105-116.
6. Zemmour D, Pratama A, Loughhead SM, *et al*. Flicr, a long noncoding RNA, modulates Foxp3 expression and autoimmunity. *Proc Natl Acad Sci U S A* 2017; **114:** E3472-E3480.
7. Carbone F, De Rosa V, Carrieri PB, *et al*. Regulatory T cell proliferative potential is impaired in human autoimmune disease. *Nat Med* 2014; **20:** 69-74.
8. Plaza-Sirvent C, Schuster M, Neumann Y, *et al*. c-FLIP expression in Foxp3-expressing cells is essential for survival of regulatory T cells and prevention of autoimmunity. *Cell Rep* 2017; **18:** 12-22.
9. Fulton RB, Meyerholz DK, Varga SM. $Foxp3^+$ CD4 regulatory T cells limit pulmonary immunopathology by modulating the CD8 T cell response during respiratory syncytial virus infection. *J Immunol* 2010; **185:** 2382-2392.
10. Lee DCP, Harker JAE, Tregoning JS, *et al*. $CD25^+$ natural regulatory T cells are critical in limiting innate and adaptive immunity and resolving disease following respiratory syncytial virus infection. *J Virol* 2010; **84:** 8790-8798.
11. Suvas S, Kumaraguru U, Pack CD, *et al*. $CD4^+CD25^+$T cells regulate virus-specific primary and memory $CD8^+$ T cell responses. *J Exp Med* 2003; **198:** 889-901.
12. Lund JM, Hsing L, Pham TT, *et al*. Coordination of early protective immunity to viral infection by regulatory T cells. *Science* 2008; **320:** 1220-1224.
13. Betts RJ, Prabhu N, Ho AW, *et al*. Influenza A virus infection results in a robust, antigen-responsive, and widely disseminated $Foxp3^+$ regulatory T cell response. *J Virol* 2012; **86:** 2817-2825.
14. Bedoya F, Cheng GS, Leibow A, *et al*. Viral antigen induces differentiation of $Foxp3^+$ natural regulatory T cells in influenza virus-infected mice. *J Immunol* 2013; **190:** 6115-6125.
15. Brincks EL, Roberts AD, Cookenham T, *et al*. Antigen-specific memory regulatory $CD4^+Foxp3^+$ T cells control memory responses to influenza virus infection. *J Immunol* 2013; **190:** 3438-3446.

16. Huehn J, Hamann A. Homing to suppress: address codes for Treg migration. *Trends Immunol* 2005; **26:** 632-636.
17. van der Veeken J, Gonzalez AJ, Cho H, *et al*. Memory of Inflammation in Regulatory T Cells. *Cell* 2016; **166:** 977-990.
18. Short KR, Kroeze E, Fouchier RAM, *et al*. Pathogenesis of influenza-induced acute respiratory distress syndrome. *Lancet Infect Dis* 2014; **14:** 57-69.
19. La Gruta NL, Kedzierska K, Stambas J, *et al*. A question of self-preservation: immunopathology in influenza virus infection. *Immunol Cell Biol* 2007; **85:** 85-92.
20. Antunes I, Kassiotis G. Suppression of innate immune pathology by regulatory T cells during Influenza A virus infection of immunodeficient mice. *J Virol* 2010; **84:** 12564-12575.
21. Moser EK, Hufford MM, Braciale TJ. Late engagement of CD86 after influenza virus clearance promotes recovery in a FoxP3$^+$ regulatory T cell dependent manner. *PLoS Pathog* 2014; **10:** e1004315.
22. Booth NJ, McQuaid AJ, Sobande T, *et al*. Different proliferative potential and migratory characteristics of human CD4$^+$ regulatory T cells that express either CD45RA or CD45RO. *J Immunol* 2010; **184:** 4317-4326.
23. Thornton AM, Piccirillo CA, Shevach EM. Activation requirements for the induction of CD4$^+$CD25$^+$ T cell suppressor function. *Eur J Immunol* 2004; **34:** 366-376.
24. Ochando JC, Yopp AC, Yang Y, *et al*. Lymph node occupancy is required for the peripheral development of alloantigen-specific Foxp3$^+$ regulatory T cells. *J Immunol* 2005; **174:** 6993-7005.
25. Fisson S, Darrasse-Jeze G, Litvinova E, *et al*. Continuous activation of autoreactive CD4$^+$CD25$^+$ regulatory T cells in the steady state. *J Exp Med* 2003; **198:** 737-746.
26. Suffia I, Reckling SK, Salay G, *et al*. A role for CD103 in the retention of CD4$^+$CD25$^+$ Treg and control of Leishmania major infection. *J Immunol* 2005; **174:** 5444-5455.
27. Huehn J, Siegmund K, Lehmann JC, *et al*. Developmental stage, phenotype, and migration distinguish naive- and effector/memory-like CD4$^+$ regulatory T cells. *J Exp Med* 2004; **199:** 303-313.
28. Teijaro JR, Walsh KB, Cahalan S, *et al*. Endothelial cells are central orchestrators of cytokine amplification during influenza virus infection. *Cell* 2011; **146:** 980-991.
29. D'Elia RV, Harrison K, Oyston PC, *et al*. Targeting the "cytokine storm" for therapeutic benefit. *Clin Vaccine Immunol* 2013; **20:** 319-237.
30. Liu Q, Zhou YH, Yang ZQ. The cytokine storm of severe influenza and development of immunomodulatory therapy. *Cell Mol Immunol* 2016; **13:** 3-10.
31. Julkunen I, Melen K, Nyqvist M, *et al*. Inflammatory responses in influenza A virus infection. *Vaccine* 2000; **19 Suppl 1:** S32-S37.

32. Fletcher JM, Lonergan R, Costelloe L, *et al*. CD39^{+}Foxp3^{+} regulatory T cells suppress pathogenic Th17 cells and are impaired in multiple sclerosis. *J Immunol* 2009; **183:** 7602-7610.

33. Ferrari D, Pizzirani C, Adinolfi E, *et al*. The P2X7 receptor: a key player in IL-1 processing and release. *J Immunol* 2006; **176:** 3877-3883.

34. McGill J, Van Rooijen N, Legge KL. Protective influenza-specific CD8 T cell responses require interactions with dendritic cells in the lungs. *J Exp Med* 2008; **205:** 1635-1646.

35. Matheu MP, Othy S, Greenberg ML, *et al*. Imaging regulatory T cell dynamics and CTLA4-mediated suppression of T cell priming. *Nat Commun* 2015; **6:** 7219.

36. Bolton HA, Zhu EH, Terry AM, *et al*. Selective Treg reconstitution during lymphopenia normalizes DC costimulation and prevents graft-versus-host disease. *J Clin Invest* 2015; **125:** 3627-3641.

37. Chen J, Ganguly A, Mucsi AD, *et al*. Strong adhesion by regulatory T cells induces dendritic cell cytoskeletal polarization and contact-dependent lethargy. *J Exp Med* 2017; **214:** 327-338.

38. Surls J, Nazarov-Stoica C, Kehl M, *et al*. Differential effect of CD4^{+}Foxp3^{+} T-regulatory cells on the B and T helper cell responses to influenza virus vaccination. *Vaccine* 2010; **28:** 7319-7330.

39. Lin PH, Wong WI, Wang YL, *et al*. Vaccine-induced antigen-specific regulatory T cells attenuate the antiviral immunity against acute influenza virus infection. *Mucosal Immunol* 2018; **11:** 1239-1253.

40. Tamura S, Ainai A, Suzuki T, *et al*. Intranasal inactivated influenza vaccines: a reasonable approach to improve the efficacy of influenza vaccine? *Jpn J Infect Dis* 2016; **69:** 165-179.

41. Zens KD, Chen JK, Farber DL. Vaccine-generated lung tissue-resident memory T cells provide heterosubtypic protection to influenza infection. *JCI Insight* 2016; **1:** e85832.

42. Fontenot JD, Rasmussen JP, Williams LM, *et al*. Regulatory T cell lineage specification by the forkhead transcription factor FoxP3. *Immunity* 2005; **22:** 329-341.

43. Hou S, Doherty PC, Zijlstra M, *et al*. Delayed clearance of Sendai virus in mice lacking class I MHC-restricted CD8^{+} T cells. *J Immunol* 1992; **149:** 1319-1325.

Figure Legends

Figure 1. mTregs exhibit distinct expression of peripheral migration- and suppression-associated markers. (**a**) nTregs (CD4^{+}eGFP^{+}CD44^{-}CD62L^{+}) and nmTregs (CD4^{+}eGFP^{+}CD44^{+}CD62L$^{-/low}$) from naïve B6-Foxp3^{eGFP} mice and mTregs (CD4^{+}eGFP^{+}CD44^{+}CD62L$^{-/low}$) from memory B6-Foxp3^{eGFP} mice were FACS-analyzed for their expression of a panel of surface and intracellular makers including CD25, CD39, CD69, CD103, CTLA-4, LFA-1, PD-1, and Foxp3. Histogram (**b**) and MFI (**c**) depict the expression of CD25, CD39, CD69, CD103, CTLA-4, LFA-1, PD-1, and Foxp3 by nTregs (grey), nmTregs (black dashed) and mTregs (black). Data represent one of three

independent experiments, each with n ≥ 6 mice per group. ns means not significant; *$P < 0.05$; **$P < 0.01$; ***$P < 0.001$; ****$P < 0.0001$.

Figure 2. mTregs are more responsive to IAV-infected APC than nTregs *in vitro*. nTregs and mTregs were FACS-sorted from naïve and memory B6-Foxp3eGFP mice, respectively, with n ≥ 6 mice per group. (**a**) Ki67 expressing cells among unstimulated or IAV-stimulated nTregs and mTregs. nTregs and mTregs were co-cultured with (stimulated) or without (unstimulated) PR8-infected BMDC for 72h followed by flow cytometric analysis of $Ki67^+$ cells. (**b**) Co-culture of nTregs and mTregs with PR8-infected BMDCs. A mixture (1:1 ratio) of nTregs (red) and mTregs (green) were co-cultured with PR8-infected BMDCs. 12 h after co-culture, a series of images was taken at 1 min intervals. Yellow open and filled arrows trace two nTregs, respectively; and blue open and filled arrows trace two mTregs, respectively. Scale bars, 20,000nm. Data represent one of three independent experiments. ns means not significant; ****P < 0.001*.

Figure 3. IAV infection selectively triggers a vigorous activation, proliferation and migration of mTregs at and to the infection site. (**a and b**) Experimental design schematic (**a**) and flow cytometric gating strategy (**b**). nTregs and mTregs were FACS-sorted from naïve C57BL/6 and memory C57BL/6-$Foxp3^{eGFP}$ mice, respectively, and then 1:1 co-transferred into naïve Ly5.1 mice. Flow cytometric gating strategy for analyzing the frequency and total number of transferred nTregs and mTregs from the recipient mice at 10 dpi. Tregs from the recipient mice were gated by using a $Foxp3^+CD25^+$ gate followed by identification of the adoptively transferred nTregs and mTregs based on the expression of congenic markers, CD45.1, CD45.2, and the reporter green fluorescent protein, eGFP. (**c**) The frequency of $Ki67^+$ cells within the adoptively transferred nTregs and mTregs in the spleens, pLNs, mLNs, BALs and lungs of recipients at 10 dpi. (**d** and **e**) The frequency (**d**) and total number (**e**) of the adoptively transferred nTregs ($eGFP^-$, grey symbols) and mTregs ($eGFP^+$, black symbols) in the spleens, pLNs, mLNs, BALs and lungs of recipients at 9 dpi. Data are representative of three independent experiments, each with n = 5 mice per group. ns means not significant; *$P < 0.05$; **$P < 0.01$; ***$P < 0.001$; ****$P < 0.0001$.

Figure 4. mTregs display enhanced suppression on the proliferation of IAV-specific $CD4^+$ and $CD8^+$ T cells. (**a** and **b**) *In vitro* proliferation of unstimulated or PR8-infected BMDCs-stimulated IAV-specific $CD4^+$ (**a**) and $CD8^+$ (**b**) T cell lines. The proliferation of IAV-specific $CD4^+$ and $CD8^+$ T cells were assessed by CFSE dilution on day 5 and day 4 after co-culture, respectively. Histograms show the CFSE dilution in both unstimulated and stimulated IAV-specific $CD4^+$ and $CD8^+$ T cells (**a** and **b**, left panels). The proliferation rates show the percentage of cells that had diluted CFSE (a and b, right panels). (**c**) *In vitro* suppression of IAV-specific $CD4^+$ and $CD8^+$ T cell proliferation by nTregs and mTregs. IAV-specific $CD4^+$ (left panel) and $CD8^+$ (right panel) T cells were co-cultured with graded nTreg (grey dashed lines) or mTreg (black dashed lines) numbers in the presence of PR8-infected BMDCs. The

suppression on the proliferation of IAV-specific $CD4^+$ and $CD8^+$ T cells by nTregs or mTregs were assessed on day 5 and day 4 after co-culture, respectively. The suppression rate represents the capacity of nTregs or mTregs to inhibit the proliferation of IAV-specific $CD4^+$ and $CD8^+$ T cells. Data represent one of three independent experiments. *$P < 0.05$; **$P < 0.01$; ***$P < 0.001$; ****$P < 0.0001$.

Figure 5. mTregs actively down-regulate CD40 and CD86 expression on BMDCs. (**a** and **b**) Expression of CD40 and CD86 on BMDCs. Immature BMDCs were co-cultured with $CD4^+$ T cells or a mix of two populations ($CD4^+$ T/nTregs or $CD4^+$ T/mTregs) at a 1:1 ratio for 24 h in the presence of IAV followed by flow cytometric analysis of CD40 and CD86 expression. As the control, immature BMDCs alone were also cultured in the presence of IAV under the same conditions. Histograms (**a**) and bar graphs (**b**) show the expression and MFI of CD40 and CD86. Data represent one of three independent experiments. *$P < 0.05$; ****$P < 0.0001$.

Figure 6. Adoptive transfer of mTregs, but not nTregs, prior to IAV infection results in marked attenuation in infection-induced body weight loss and lung damage. nTregs or mTregs were adoptively transferred into Ly5.1 recipient mice 12 h before intranasal PR8 infection. (**a**) Body weight of PBS-injected (Control), PR8-infected (Infected only), adoptively transferred nTregs plus PR8-infected (Infected + nTregs) and adoptively transferred mTregs plus PR8-infected (Infected + mTregs) mice. Body weight changes were monitored daily after PR8 infection. Depicted *P*-value corresponds to comparison of "Infected only" with "Infected + mTregs". The difference between "infected only" and "Infected + nTregs" was not statistically significant. These data are representative of more than three independent experiments. (**b** and **c**) Histopathological analysis of the lungs from control, infected only, "Infected + nTregs" and "Infected + mTregs" mice on day 10 post PBS or PR8 inoculation. (**b**) Representative H&E stained histological lung tissue sections. (**c**) Quantification of infiltration rate (left) measured by Fiji imageJ and extent of tissue damage (right) scored according to infiltration rate. These data represent one of three independent experiments ($n \geq 5$ mice per group). ns means not significant; *$P < 0.05$; **$P < 0.01$; ***$P < 0.001$; ****$P < 0.0001$.

Supplementary figure 1. mTregs are bigger in size and making more contact with IAV-infected BMDCs. nTregs and mTregs were FACS-sorted from naïve and memory B6-$Foxp3^{eGFP}$ mice, respectively, with $n \geq 6$ mice per group. (**a and b**) A mixture (1:1 ratio) of nTregs and mTregs were co-cultured with PR8-infected BMDCs. 12 h after co-culture, a series of images was taken at 1 min intervals, followed by quantitating cell size (**a**) and average Treg-DC contacting time (**b**) were analyzed using Fiji ImageJ software. Data represent one of three independent experiments. ns means not significant; *$P < 0.05$; **$P < 0.01$; ***$P < 0.001$.

Supplementary figure 2. nTregs and mTregs activation triggered by anti-CD3/CD28 antibodies. Ki67 expressing cells among unstimulated or anti-CD3/CD28 antibodies-stimulated nTregs and mTregs. nTregs and mTregs were

co-cultured with BMDCs for 72h in the absence or presence of anti-CD3/CD28 antibodies prior to the flow cytometric analysis of $Ki67^+$ cells. Data represent one of three independent experiments. ns means not significant.

Supplementary figure 3. mTregs are activated to proliferate and migrate *in vivo* specifically by IAV infection. $1x10^6$ FACS-purified mTregs from memory C57BL/6-$Foxp3^{eGFP}$ mice were adoptively transferred into congenic Ly5.1 mice. The recipient mice were intranasally inoculated with PBS or PR8 and sacrificed on day 10 post PBS- or PR8-inoculation. (**a**) The percentage of $Ki67^+$ cells among the adoptively transferred total mTregs recovered in the spleens, pLNs, mLNs and lungs of PBS treated (black symbols) or PR8 infected (grey symbols) recipients. (**b**) Total number of adoptively transferred mTregs in the spleens, pLNs, mLNs and lungs of PBS treated or PR8 infected recipients. Data are representative of three independent experiments, each with $n \geq 4$ mice per group. ns means not significant; $*P < 0.05$; $**P < 0.01$; $***P < 0.001$; $****P < 0.0001$.

Supplementary figure 4. IAV infection and co-culture with nTregs or mTregs does not result in marked change in the expression of CD40 and CD86 on BMDCs. (**a** and **b**) Expression of CD40 and CD86 on IAV-infected BMDCs. Immature BMDCs were cultured in the absence or presence of IAV for 24 h; alternatively, immature BMDCs were co-cultured with nTregs or mTregs in the presence of IAV for 24 h; the expression of CD40 and CD86 on BMDCs were then FACS-analyzed. Histograms (**a**) and bar graphs (**b**) show the expression and MFI of CD40 and CD86. Data are representative of three independent experiments. ns means not significant.

Supplementary figure 5. mTregs actively limit the infiltration of monocytes, neutrophils and IFN-γ-secreting $CD4^+$ and $CD8^+$ T cells into the infected lungs. nTregs or mTregs were adoptively transferred into Ly5.1 recipient mice 12 h before intranasal PR8 infection. Ly5.1 recipient mice were sacrificed at 10 dpi and cells in the lungs were isolated and stained for monocytes ($CD11b^+Ly6C^+$), interstitial macrophages ($CD11b^+Siglec\text{-}F^{low/-}$) and neutrophils ($CD11b^+Ly6G^+$). Alternatively, the IFN-γ-secreting $CD4^+$ ($CD4^+Foxp3^-INF\text{-}\gamma^+$) and $CD8^+$ ($CD8^+INF\text{-}\gamma^+$) T cells were analyzed after peptide stimulation. (**a-e**) Total number of infiltrating monocytes (**a**), interstitial macrophages (**b**), neutrophils (**c**), IFN-γ-secreting $CD4^+$ (**d**) and $CD8^+$ (**e**) T cells in the lungs of PBS-injected (Control), PR8-infected (Infected only), adoptively transferred nTregs plus PR8-infected (Infected + nTregs) and adoptively transferred mTregs plus PR8-infected (Infected + mTregs) mice. Data are representative of three independent experiments ($n \geq 4$ mice per group). ns means not significant; $*P < 0.05$; $**P < 0.01$; $***P < 0.001$; $****P < 0.0001$.

Figure 1

imcb_12271_f1-6.pdf

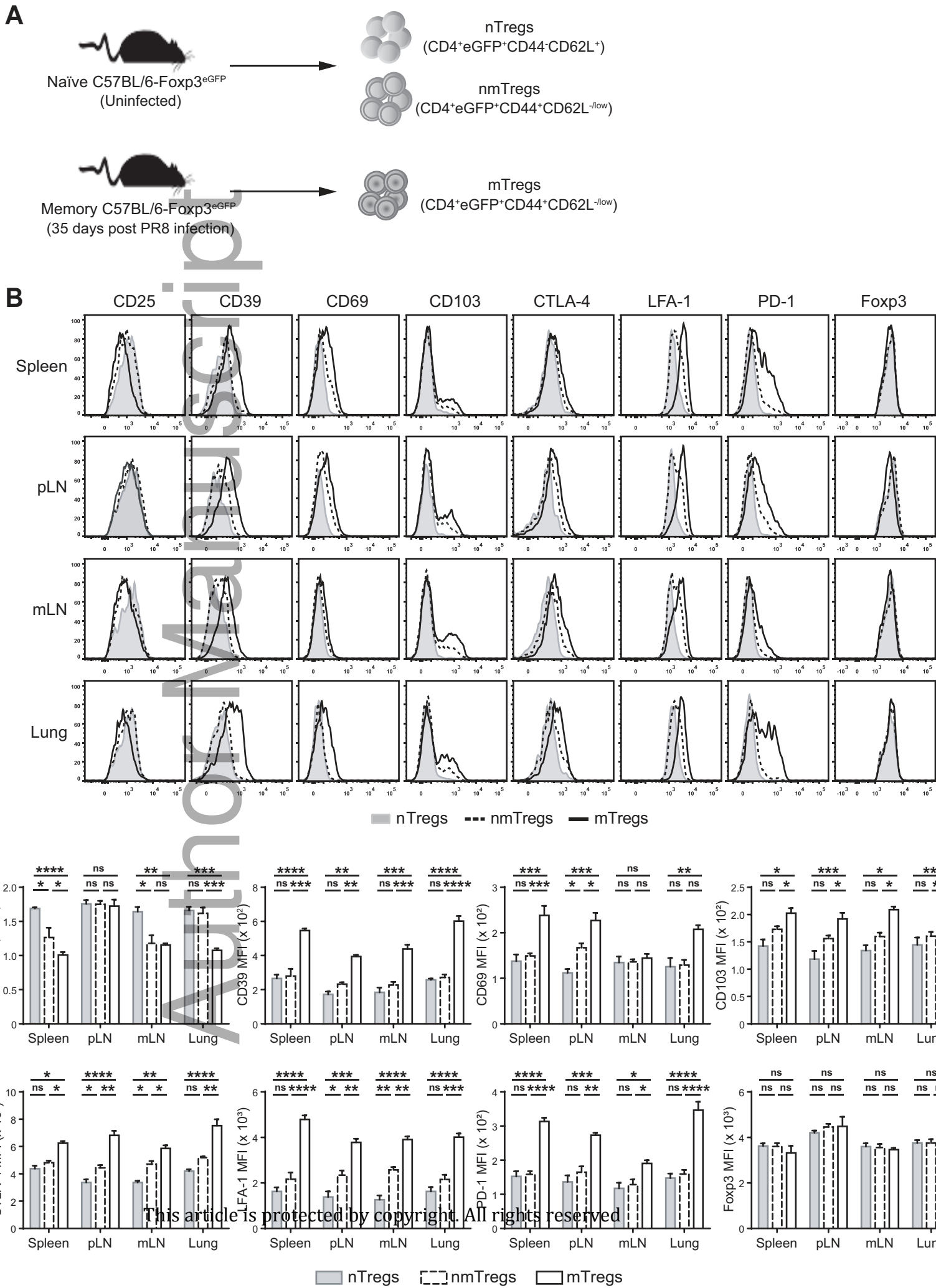

Figure 2

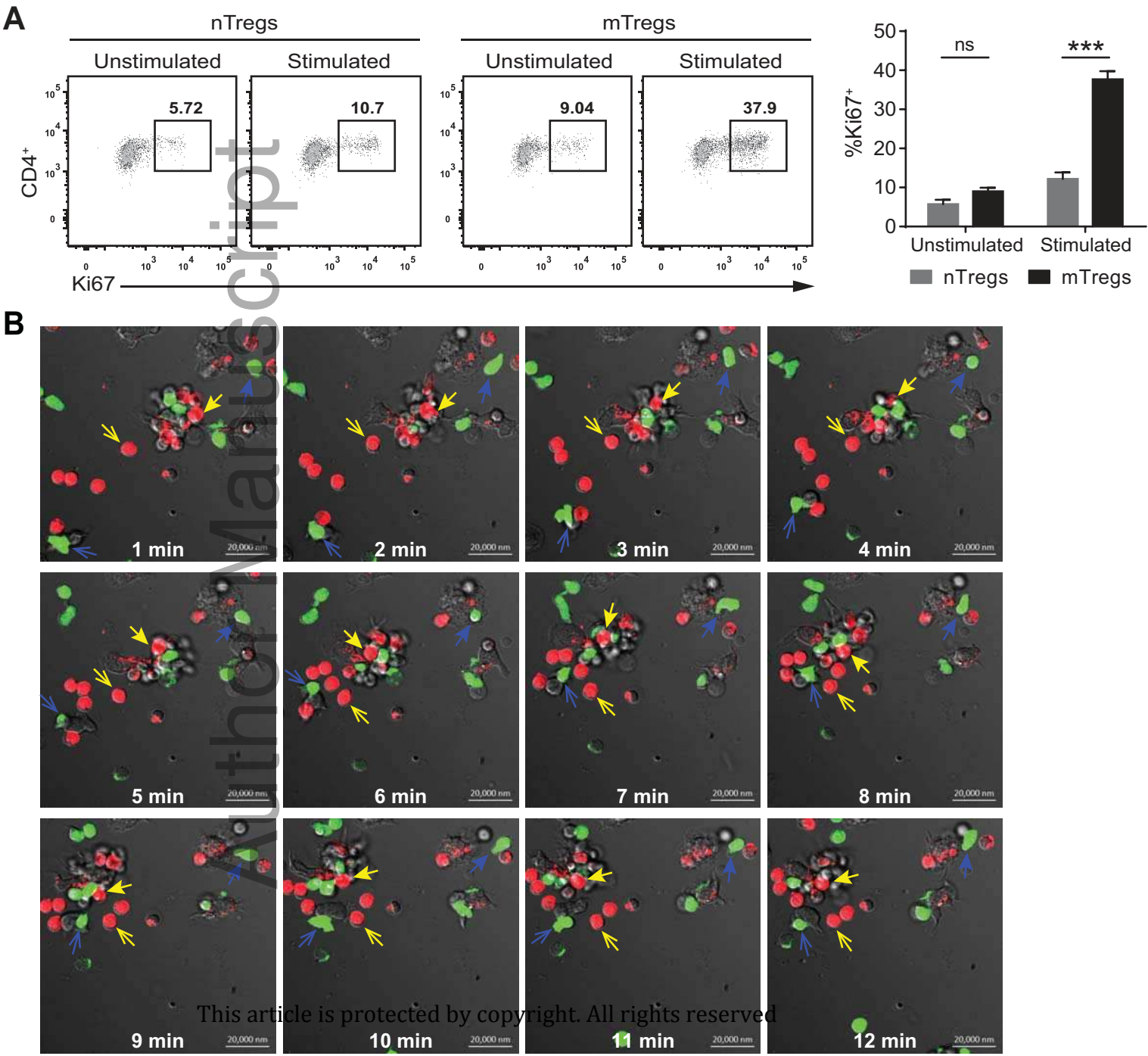

Figure 3

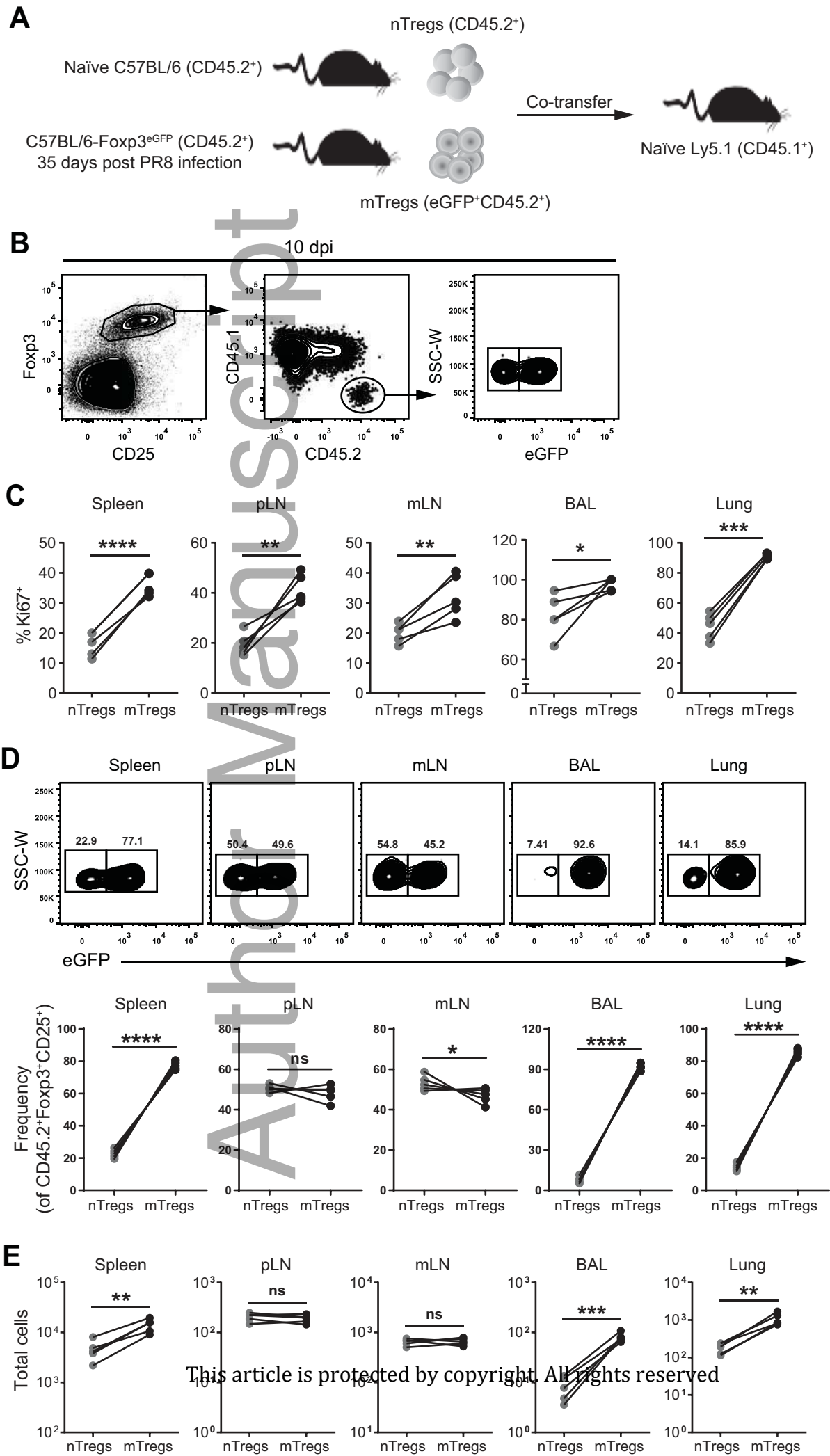

Figure 4

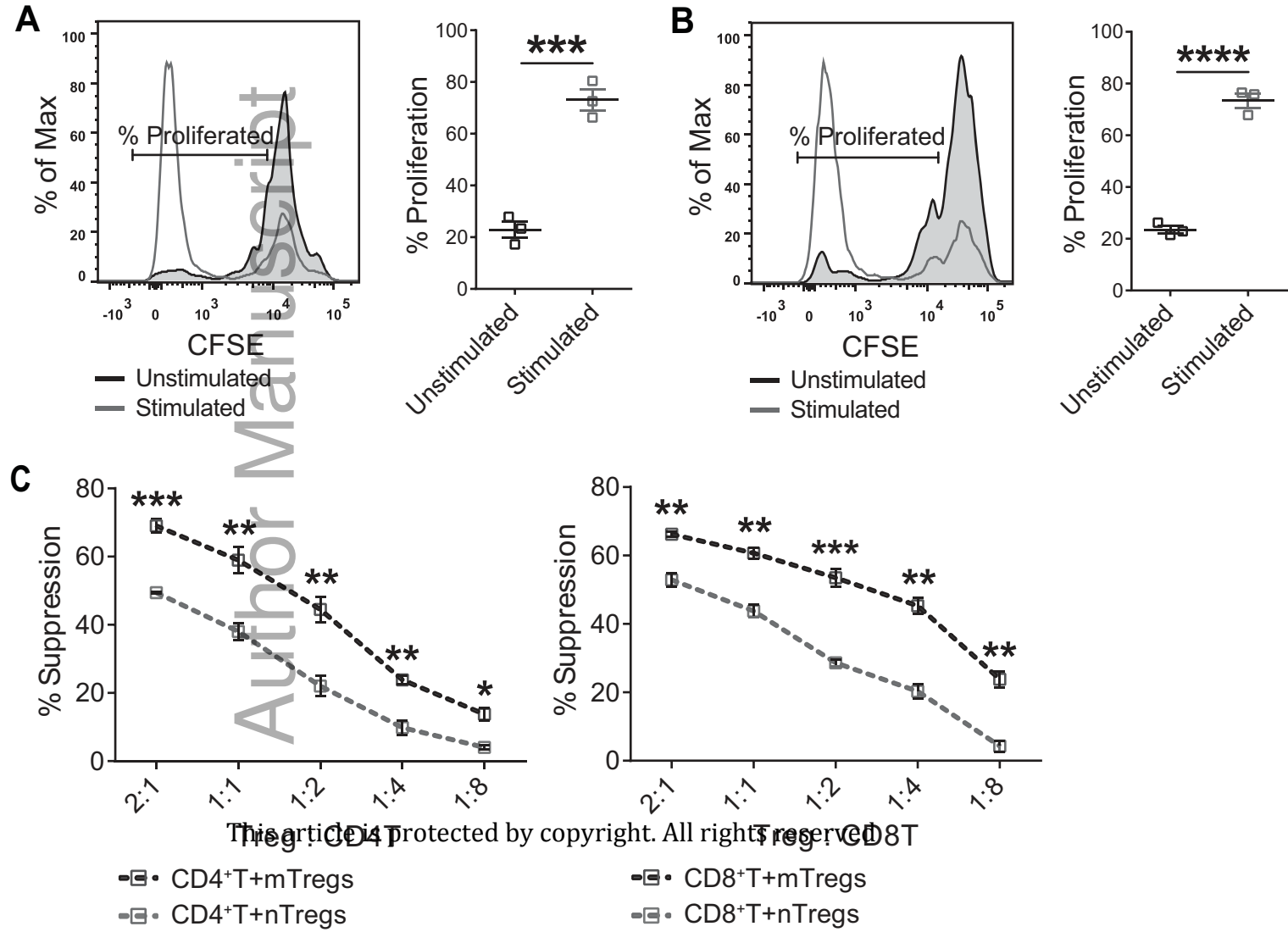

Figure 5

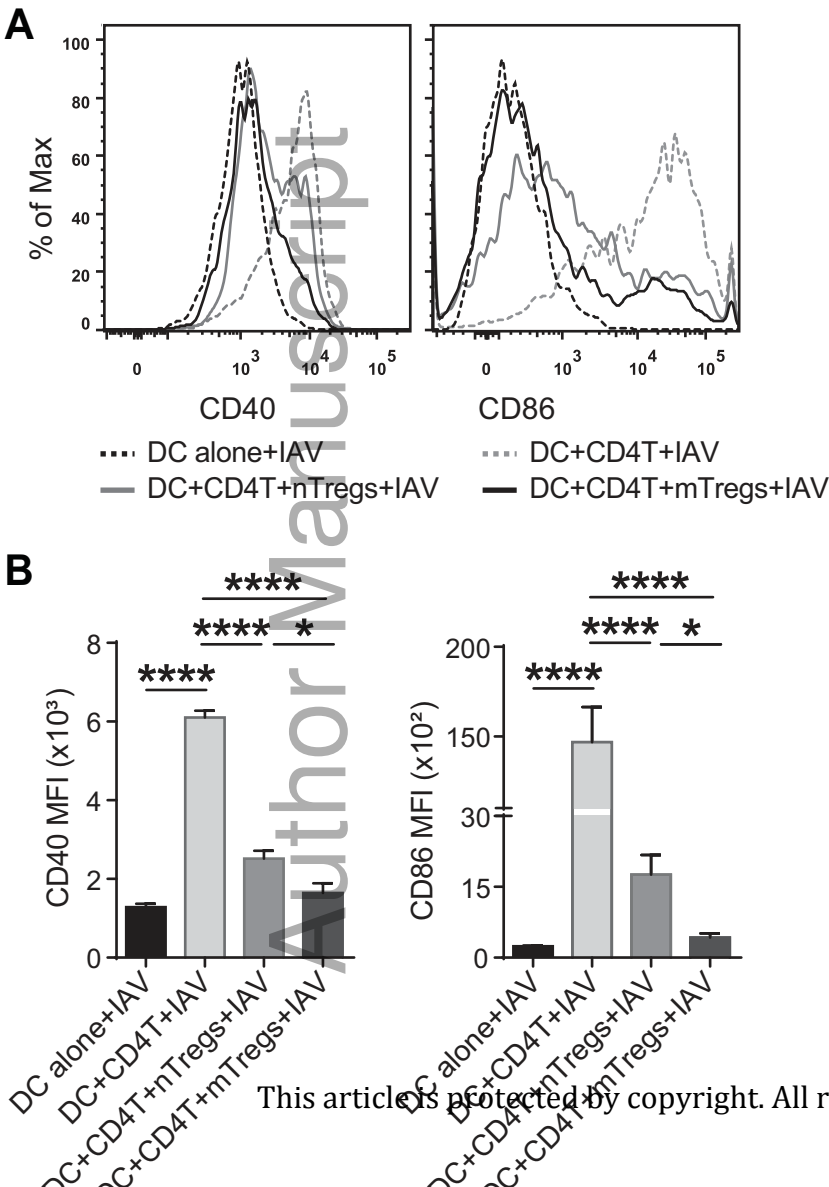

Figure 6

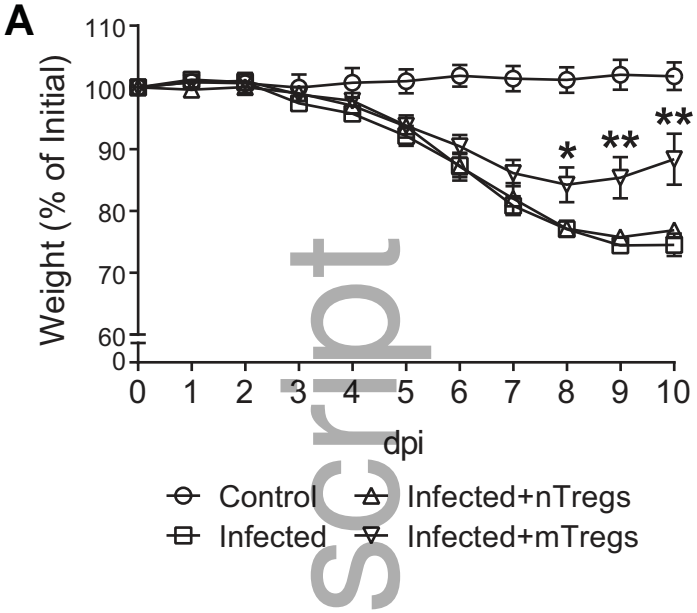

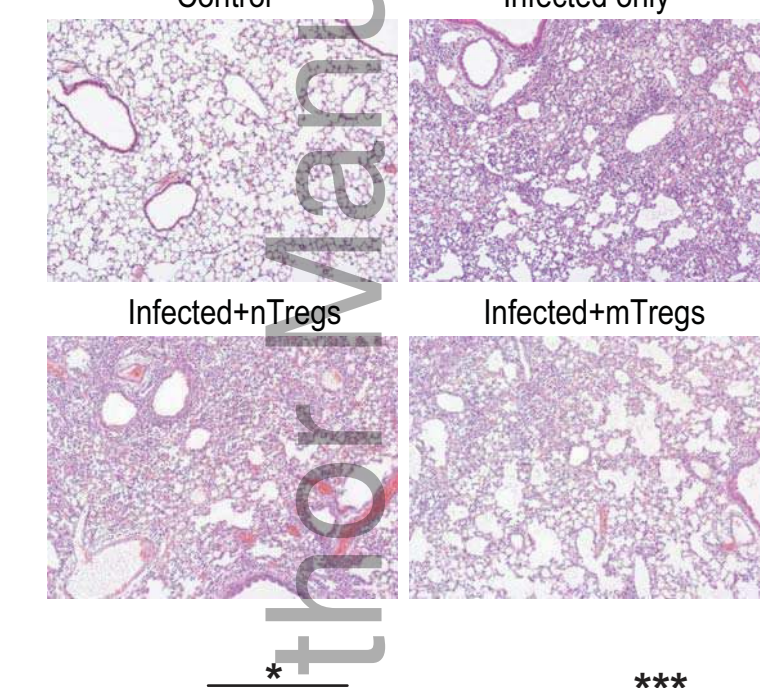

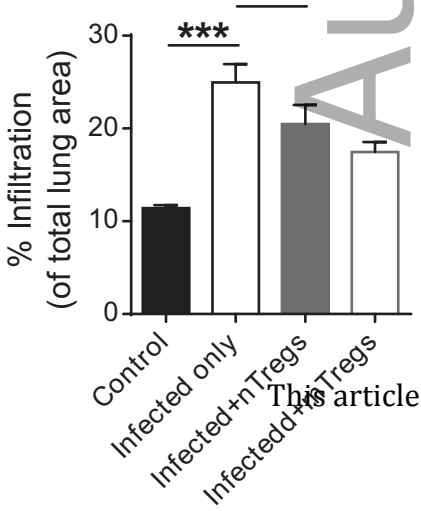

Author/s:
Lu, C;Zanker, D;Lock, P;Jiang, X;Deng, J;Duan, M;Liu, C;Faou, P;Hickey, MJ;Chen, W

Title:
Memory regulatory T cells home to the lung and control influenza A virus infection.

Date:
2019-10

Citation:
Lu, C., Zanker, D., Lock, P., Jiang, X., Deng, J., Duan, M., Liu, C., Faou, P., Hickey, M. J. & Chen, W. (2019). Memory regulatory T cells home to the lung and control influenza A virus infection.. Immunol Cell Biol, 97 (9), pp.774-786. https://doi.org/10.1111/imcb.12271.